https://dx.doi.org/10.1016/j.tra.2024.104005

An emission control policymaking model for sustainable river transportation

Lu Zhen[1], Shuanglu Zhang[1], Dan Zhuge[1*], Shuaian Wang[2], Yong Wang[3]

[1]*School of Management, Shanghai University, Shanghai, China*
[2]*Department of Logistics and Maritime Studies, The Hong Kong Polytechnic University, Kowloon, Hong Kong*
[3] *School of Economics and Management, Chongqing Jiaotong University, Chongqing, China*

* Corresponding author: dan_zhuge@shu.edu.cn

Abstract: Sustainable river transportation is an important component in the development of green transportation. Emission control policymaking in rivers is a key measure for realizing sustainable river transportation. Transportation demand for an origin–destination pair of cities along a river may involve transferring between land transportation and water transportation. This study takes this into account by using a mathematical programming methodology to propose a model for emission control policymaking for sustainable river transportation that minimizes the total emissions produced by both land transportation and river transportation. The model supports government regulators in making heterogeneous emission control area (ECA) policies for a river, which is shown to be superior to a traditional homogeneous ECA policy. A branch-and-bound algorithm is also developed to solve the model. Using two of China's main rivers, a case study is conducted to derive computational results that may be potentially useful for government regulators in policymaking.

Keywords: Emission control; model for policymaking; sustainable river transportation; mixed-integer linear programming; branch and bound.

1. Introduction

River transportation plays a central role in merchandise trade and cargo transportation. Waterway freight transportation is more environmentally friendly than other transportation modes (e.g., land transportation). However, frequent river transportation activities generate considerable amounts of pollutant gases, especially sulfur oxides (SO_x) emissions, which have a significant impact on the environment of port cities (Wang et al., 2021). Considering the high population density of port cities, both academia and industry have paid increasing attention to human health problems caused by SO_x emissions, including respiratory symptoms, lung disease, and premature death. To control air emissions from shipping, the sustainability of river transportation has become an important issue in the establishment of green, low-emission social development.

To achieve sustainable river transportation, many countries and organizations have implemented emission control policies, e.g., the compulsory use of shore power and the use of the Energy Efficiency Operational Index. One of the most important policies has been the establishment of emission control areas (ECAs) with a 0.1% sulfur limit. Four international ECAs—the North American area, the Baltic

Sea area, the North Sea area, and the United States Caribbean Sea area—have been established since January 2015. Four South Korean ports—Incheon, Pyeongtaek-Dangjin area, Yeosu, Gwangyang area, Busan area, and Ulsan area—have also been designated as ECAs since January 2022. China has enforced a 0.1% sulfur emission limit for its inland rivers since January 2020. Although the effectiveness of ECAs in reducing shipping emissions has been confirmed by Svindland (2018) and Zhang et al. (2020), the choice of the sulfur limit and boundary width for each traditional homogeneous ECA is rather subjective and can be further optimized. It should be noted that an emission control policy that is too strict will lead to a dramatic increase in river transportation costs, thus causing a modal shift from river transportation to land transportation. Transporting one unit of cargo per kilometer by river usually consumes less fuel and produces fewer emissions than doing the same by land. As a result, if emission control policies for river transportation are too strict, higher total emissions may result as operators shift to land transportation. Therefore, government regulators need a more scientific method to formulate emission control policies for river transportation. By using a more scientific approach to policymaking models, government regulators can establish more precise emission control policies. For example, in different areas of a river, sulfur caps can be set at different limits. This is what we propose in this study. We refer to setting sulfur caps at different limits as a "heterogeneous" ECA policy. The proposed ECA policy is superior to the traditional homogeneous ECA policy from a theoretical perspective.

This study explores the application of mathematical programming to policymaking for sustainable river transportation. It proposes a novel idea of heterogeneous emission control policymaking for river transportation, and formulates a mixed-integer linear programming (MILP) model to decide the policy for the degree of sulfur emission control (i.e., sulfur caps) in all areas of a river. The objective of the MILP model is to minimize total emissions from both land transportation and river transportation while fulfilling all of the transportation demands of origin–destination (OD) pairs along the river. Tactics are applied to linearize the model. A branch-and-bound algorithm is then developed to solve the model. Some potentially useful managerial insights are also derived to support policymaking at the side of government regulators who are responsible for building sustainable river transportation systems.

The remainder of this paper is organized as follows. The related literature is reviewed in Section 2. A detailed description of the heterogeneous ECA design for rivers is provided in Section 3. Then the MILP model and the branch-and-bound algorithm are designed in Section 4 and Section 5, respectively. Using the proposed model and algorithm, a case study for two representative rivers in China is conducted in Section 6. Finally, the conclusions are outlined in Section 7.

2. Related studies

Sustainable transport has become a major concern in recent years (Zis, 2019; Kong et al., 2021; Ling et al., 2022; Gao et al., 2023). This study focuses on applying optimization models for emission control policymaking for sustainable river transportation. Related studies are thus reviewed from the following three streams of research: studies related to emission control for shipping, optimization-based methodology for policymaking, and studies related to operations research on green river shipping.

The first stream of research involves studies related to emission control for shipping. ECA policy has recently become one of the most important issues for sustainable transportation. This is especially so in water transportation because the unit emission of ships is much greater than that of cars and other vehicles. ECA-related topics have received considerable attention from academics and practitioners. Chang et al. (2014) compared ECAs with speed reduction zones and concluded that ECAs can reduce SO_2 emissions more effectively. The efficacy of ECAs in mitigating SO_2 emissions was also validated by Svindland (2018) and Zhang et al. (2020). Zhen et al. (2020) discussed the impacts of fuel cost, decision makers, and ECA boundaries on shipping emissions. Joseph et al. (2021) presented a techno-economic environmental cost model under two policy scenarios—an Arctic zero emission ECA policy scenario and a business-as-usual policy scenario. They found that summer Arctic and winter Suez transits were financially viable under both policy scenarios while noting that the implicit damage costs of shipping emissions could not be overlooked. Tan et al. (2022b) investigated ship's detour decision under an ECA regulation. They presented a voyage cost minimization model considering the relative position between the ports and the ECA boundary, and the fuel price ratio of VLSFO (very low sulfur fuel oil) and MGO (marine gas oil). They analyzed detour behavior in the coastal ECAs of China and the US based on the proposed model and discussed the economic and environmental effects caused by such detour behavior. Liu et al. (2023) addressed a ship emission monitoring problem in ECAs involving unmanned aerial vehicles. They proposed an MILP model based on a time–space network, and solved the model by developing an exact method, including structure enumeration, column generation, and row generation.

The second stream of research involves optimization-based methods for policymaking. Policymaking decisions are usually made according to the decision makers' experience, many complex factors, and implicit knowledge that is hard to express explicitly. Thus, it is not easy to establish mathematical models for policymaking. However, policymaking based on mathematical models has become an interesting (and also challenging) direction for academia. Studies have proposed an increasing number of optimization models for policymaking in specific domains. Zis et al. (2019) examined different policy options that can reverse modal shifts caused by stricter regulation of sulfur emissions based on

the generalized cost of transport, modal choice, and a road network model. Sun et al. (2020) developed an MILP model to determine the location of ECAs. Zhuge et al. (2021) presented two Stackelberg game models to design suitable subsidies in a vessel speed reduction incentive program under different government policies—no government intervention, a sharing subsidy policy, and an air emission tax policy. Meng et al. (2022) proposed a tripartite evolutionary game model to choose the optimal carbon emission reduction strategy. Three parties—the government, ports, and shipping companies—were involved in the proposed model. Their results provide policy recommendations for reducing carbon emissions in maritime transportation. Gong and Li (2022) analyzed sulfur emission control policies for liner shipping on the Maritime Silk Road and the subsidy for China–Europe Railway Express. They then developed two welfare maximization models to determine the optimal sulfur emission control coverage and the optimal subsidy. Zhen et al. (2022) focused on a ship-borne power receiving system deployment problem. They presented a nonlinear programming model to compare the effect on the problem of an incentive policy based on berthing priority and an incentive policy based on government subsidies. Chua et al. (2023) constructed a fleet planning model to investigate the effect of an emissions trading system (ETS) on the decisions of shipping companies, and analyzed the effectiveness of the ETS with various policy design parameters in reducing emissions.

The last stream of research concerns studies related to operations research on green river shipping. These studies use operations research methods to improve the sustainability of river transportation from the perspective of government regulators. However, most decision makers in this line of research are river shipping companies. Yan et al. (2018) optimized the sailing speed of inland ships using a distributed parallel k-means clustering algorithm, which can reduce fuel consumption and CO_2 emissions effectively. Tan et al. (2022a) analyzed the choice between green fuel and installing scrubbers to meet sulfur emission limits on an inland river considering sailing speed. Buchem et al. (2022) investigated a speed optimization problem for inland waterway transportation with stochastic waiting times. Wang et al. (2023) discussed the effect of sailing speed on the emissions of ships subject to environmental policies on the Yangtze River. Zhang et al. (2023) established a speed and energy optimization model for inland all-electric ships in battery charging mode.

In summary, the present study combines these three research streams. Few studies have applied mathematical programming as a methodology for emissions policymaking for river transportation. Both an MILP model and an exact algorithm are designed for this cutting-edge problem. This study contributes to the literature on both green/sustainable shipping and policymaking methodology based on operations research.

3. Problem description

This section elaborates some important concepts and core assumptions that form the basis of the problem. As previously mentioned, this problem is oriented toward the design of an emission control policy for inland river transportation. Figure 1 shows a conceptual diagram for water transportation for a set of ports along a river. This study considers land transportation as the rival (alternative) mode to water transportation.

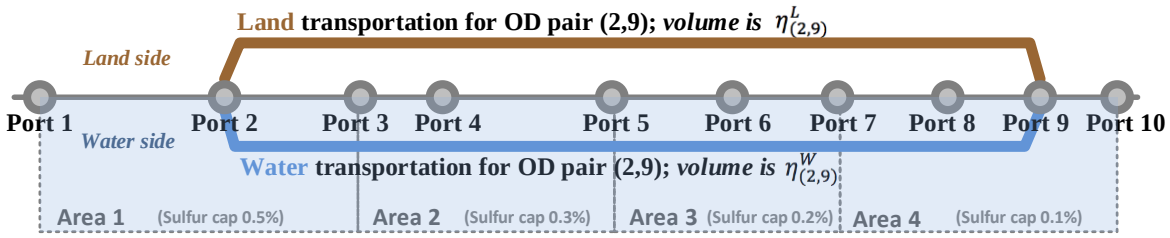

Note: Transportation demand for OD pair (2,9) $\bar{n}_{(2,9)}$ is split into two modes: $\bar{n}_{(2,9)} = \eta^W_{(2,9)} + \eta^L_{(2,9)}$

Figure 1: Conceptual diagram for water and land transportation between a pair of OD ports

For each OD pair of ports, transportation demand is given as a known parameter. This demand can be satisfied by either water transportation or land transportation. Given an OD pair, transportation demand is split between the two transportation modes according to customers' perceived value, which is an important concept defined in this study. The demand split is an important issue and has been investigated in some literature, which also investigated some factors that influence the split in practice. In this paper, we assume transportation demand is split between water and land transportation modes according to customers' perceived value, which is an important concept defined in this study. Customers' perceived value can be regarded as customers' satisfaction reflected by different services, which is an important factor affecting demand. This definition can also be used in the transportation network, whereby shippers tend to choose transportation mode based on the degree of their requirement (Duan et al., 2019; Khakdaman et al., 2020). Li and Shang (2016) investigated the modal split of passenger travel demand and find that route travel time is the most important factor affecting the market share of the air transport and high-speed railway services. Zhang et.al (2022) considered shippers' preferences can match services and demands in a better way for synchromodal transport planning problem. Cost and time are included in shippers' preferences for satisfaction calculation. Hu et.al (2022) developed the optimal subsidy schemes that maximize the waterway share in an intermodal transportation network. And shipping cost and transit time are two main concerns for intermodal demand share consideration.

For each transportation mode—land or water—customers perceive a value for transporting one unit of cargo between the two ports in an OD pair. This value can be determined according to the delivery time, unit delivery cost, and other factors. The shorter the delivery time, the lower the delivery cost, and

thus the higher the customers' perceived value. Specifically, the value can be calibrated as a weighted sum of the reciprocal of the delivery time and the reciprocal of the unit delivery cost. The reason for using the reciprocals of these factors is that the lower the values of time and cost, the higher the customers' perceived value. Given an OD pair, land transportation may have a shorter delivery time but a higher unit delivery cost, while water transportation may have a longer delivery time but a lower unit delivery cost. Customers' perceived values for the two transportation modes may then be matched. This study assumes that the transportation demand between an OD pair is split into two modes according to the ratio of the perceived value of the two modes. For example, the transportation demand between an OD pair is 1,000 TEUs if customers' perceived values for land transportation and water transportation are 40 and 60, respectively. The transportation volumes via land transportation and water transportation between the OD pair are 400 and 600 TEUs, respectively. It should be noted that when the transportation of specific cargo between an OD pair is definitely by water (or land), irrespective of the delivery time or cost, the demand for this case will not be considered in the above demand split.

As the theme of this study, an emission control policy first affects the unit delivery cost of water transportation. It then affects customers' perceived value of water transportation, and finally it affects the transportation volume split between each OD pair. Figure 1 shows that the water regions of a river or a coastal area are divided into areas that may have different emission control policies. For example, different areas may have different limits on the permitted percentage of sulfur content in bunker fuel. For the example in Figure 1, the sulfur cap in Areas 1, 2, 3, and 4 is 0.5%, 0.3%, 0.2%, and 0.1%, respectively. Here we assume that the policy for the degree of emission control in one area is identical. Thus, the concept of an area is the unit region for designing an emission control policy for water transportation.

A voyage route may cross multiple areas. In this case, a ship on a given voyage route must obey the strictest emission control policy across multiple areas. For example, a ship using the voyage route from Port 2 to Port 9 (Figure 1), must obey the sulfur cap of 0.1%, which is the strictest emission control policy of the four areas.

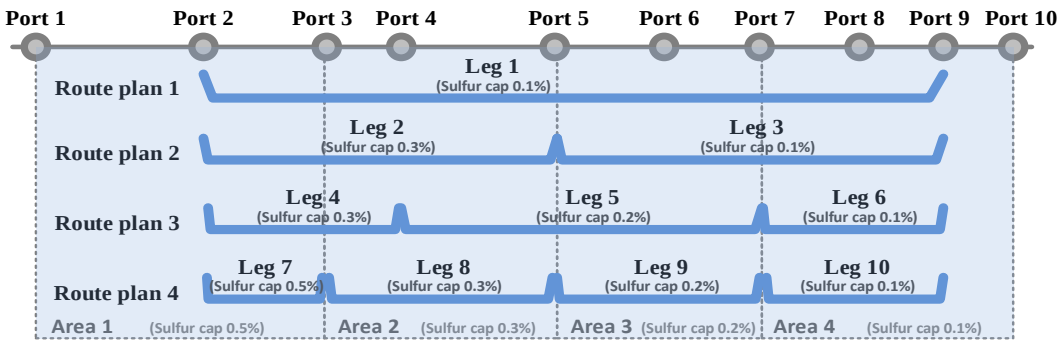

Figure 2: Multiple route plans between a pair of OD ports

It should be noted that there may be more than one route plan between an OD pair due to transshipment. For the above example in Figure 2, we assume that there are four route plans for the OD pair between Port 2 and Port 9. Each route plan may consist of one or multiple voyage legs. As mentioned, the degree of emission control that a voyage leg must obey must be the strictest of the multiple areas that the leg crosses. Therefore, a route plan may be subject to multiple policies for the degree of emission control due to transshipment. The green technology, like new energy LNG, is a promising alternative, as it offers potential cost savings in addition to replying with ECA regulations. However, the investment in retrofitting existing vessels to enable them to run on LNG comes with significant upfront costs. Moreover, the price difference between LNG and conventional marine fuels, the availability of LNG and the reliability of its supply chain remain highly uncertain. Thus, the green technology option here is not considered.

As this study focuses on the design of an emission control policy for water transportation, land transportation acts as an alternative (or rival) way to split transportation demand with that for water transportation. Therefore, we omit details of land transportation, such as transshipment, in this study. We treat customers' perceived value of land transportation with respect to one unit of cargo for each OD pair as a known parameter in this study.

Finally, the unit emission of land transportation for each OD pair and the unit emission of water transportation for each voyage leg under a specific degree of emission control are known parameters. The objective is to minimize total emissions from both land transportation and water transportation while fulfilling all of the transportation demands of OD pairs. The core decision variables are to decide the policies regarding the degree of emission control in all areas in a given water region. This affects the delivery cost of water transportation, the ratio of customers' perceived values between land transportation and water transportation, and the transportation volume split among land and the various route plans via water. Finally, it affects total emissions from both land transportation and water transportation. In the next section, we formulate a nonlinear MILP model to optimize the above decisions.

4. Basic model and analysis

Given an OD pair, the delivery times of various route plans are different due to transshipment delays involved in different plans. The delivery costs of various route plans are also not identical due to the influence of different emission control policies on the different legs contained in the plans. Customers' perceived value of water transportation along a route plan can be calibrated by aggregating the perceived values of all of the legs contained in the route plan minus the value incurred by the delivery

time delay due to transshipment activities in the route plan. The perceived value of a leg under a specific degree of emission control and the value reduction due to transshipment in a specific route plan are known parameters in this study. It is easy to understand that policy decisions on the degree of emission control in different areas influence customers' perceived value of each route plan. Recall that each OD pair may contain multiple water transportation route plans. Customers' perceived value of an OD pair is a weighted sum of the perceived values of all of the route plans for that OD pair. Here, the weight of each route plan is the percentage of the transportation volume via the route plan to the total volume for the OD pair. Therefore, this study considers both the influence of emission control policy design on demand splitting between land transportation and water transportation for a given OD pair, and water transportation demand splitting among different route plans for that OD pair.

This section first formulates a basic model for deciding the degree of emission control in areas to minimize total emissions from land transportation and water transportation among all OD pairs. As the formulated model is nonlinear, we then discuss the method for linearizing the model. At the end of this section, we also analyze some properties of the model.

4.1 Model formulation

Before formulating the model, the indices, parameters, and decision variables used in this model are elaborated as follows. To facilitate understanding of the model formulation, this paper uses Roman letters and Greek letters to denote parameters and variables, respectively.

Indices and sets

d index of the degree of emission control; the set of all degrees is D.

p index of an OD pair of transportation demand; the set of all pairs is P.

a index of an area where the policy for the degree of emission control is identical; the set of all areas is A.

y index of a route plan via water to fulfill transportation demand for an OD pair.

g index of a voyage leg; a route plan contains some connected legs; the set of all legs is G.

Y_p set of the route plans via water to fulfill transportation demand for OD pair p.

G_y set of voyage legs that constitute route plan y.

A_g set of areas related to voyage leg g.

Parameters

$\bar{n}_p$ total volume of transportation for OD pair p.

$\dot{e}_p^L$ unit emission via land transportation for OD pair p.

$\dot{e}_{gd}^W$ unit emission via water transportation for leg g under policy degree d.

v_p^L unit of customers' perceived value of land transportation for OD pair p.

v_{gd}^W unit of customers' perceived value of water transportation for leg g under policy degree d.

v_y^{-T} unit of customers' perceived value reduction due to transshipment of route plan y via water.

Decision variables

β_{ad} binary, equals one if area a is under policy degree d, and otherwise zero.

θ_{gd} binary, equals one if transportation for leg g is under policy degree d, and otherwise zero.

π_y transportation volume of route plan y via water.

γ_p^W unit of customers' perceived value of water transportation for OD pair p.

η_p^W volume via water transportation for OD pair p.

η_p^L volume via land transportation for OD pair p.

Mathematical model

[**M1**] Minimize $\sum_{p\in P}\left[\dot{e}_p^L\eta_p^L+\sum_{y\in Y_p}\pi_y\left(\sum_{g\in G_y}\sum_{d\in D}\dot{e}_{gd}^W\theta_{gd}\right)\right]$ (4-1)

s.t. $\sum_{d\in D}\beta_{ad}=1$ $\forall a\in A$ (4-2)

$\sum_{d\in D}\theta_{gd}=1$ $\forall g\in G$ (4-3)

$\max_{a\in A_g}\{\sum_{d\in D}d\beta_{ad}\}=\sum_{d\in D}d\theta_{gd}$ $\forall g\in G$ (4-4)

$\eta_p^W+\eta_p^L=\bar{n}_p$ $\forall p\in P$ (4-5)

$\sum_{y\in Y_p}\pi_y=\eta_p^W$ $\forall p\in P$ (4-6)

$\frac{\eta_p^W}{\eta_p^L}=\frac{\gamma_p^W}{v_p^L}$ $\forall p\in P$ (4-7)

$\gamma_p^W=\frac{1}{\eta_p^W}\sum_{y\in Y_p}\pi_y\left(\sum_{g\in G_y}\sum_{d\in D}v_{gd}^W\theta_{gd}-v_y^{-T}\right)$ $\forall p\in P$ (4-8)

$\beta_{ad}\in\{0,1\}$ $\forall a\in A, d\in D$ (4-9)

$\theta_{gd}\in\{0,1\}$ $\forall g\in G, d\in D$ (4-10)

$\eta_p^W,\eta_p^L,\gamma_p^W\geq 0$ $\forall p\in P$ (4-11)

$\pi_y\geq 0$ $\forall p\in P, y\in Y_p$ (4-12)

Objective (4-1) minimizes the total emission of the land and water transportation. Constraints (4-2) ensures each area is under one certain degree of emission control policy. Constraints (4-3) state each voyage leg's water transportation is executed according to one certain degree of emission control policy. Constraints (4-4) connect the above two emission control degrees in an area and a leg related to the area. As aforementioned in the previous section, a voyage leg's degree is the highest degree of the multiple areas that the voyage leg covers. Constraints (4-5) state that the transportation demand for each OD pair

p is split into the land way with volume η_p^L and the water way with volume η_p^W. Constraints (4-6) are to further split the water transportation volume η_p^W among various route plans; each one is with volume π_y. Constraints (4-7) state that the transportation demand for each OD pair is split according to the ratio of the unit customers' perceived value via the two ways. More specifically, given an OD pair p, the ratio of transportation volume via water to land (η_p^W/η_p^L) equals to the ratio of the unit customers' perceived value via water to land (γ_p^W/v_p^L). For each OD pair, the perceived value for land transportation is a parameter (i.e., v_p^L); while the value for water transportation is a variable (i.e., γ_p^W), which is calculated in Constraints (4-8). As aforementioned in the previous section, given an OD pair p, γ_p^W is a weighted sum of the perceived values of all the route plans for the OD pair ($y \in Y_p$); here the weight of each route plan could be the percentage of the transportation volume via the route plan within the total volume of the OD pair (i.e., $\pi_y/\sum_{y\in Y_p}\pi_y$). When calculating one route plan's perceived value, it equals to the sum of perceived value of all the legs contained in the route plan (i.e., $\sum_{g\in G_y}\sum_{d\in D} v_{gd}^W\theta_{gd}$) minus a value reduction incurred by the delay of the transshipment involved in the route plan (i.e., v_y^{-T}). Constraints (4-9)~(4-12) define the decision variables.

4.2 Model linearization

In the objective function, the emission via water transportation $\sum_{y\in Y_p}\pi_y\left(\sum_{g\in G_y}\sum_{d\in D}\dot{e}_{gd}^W\theta_{gd}\right)$ contains the product of the variable π_y with the variable θ_{gd}, which is nonlinear. Moreover, constraint (4-7) contains a nonlinear part $\gamma_p^W\eta_p^L$, which is the product of two continuous variables. In particular, constraint (4-4) also is nonlinear because of the max operator. To linearize these forms, we define some new variables and constraints.

Newly defined indices and sets:

B set of possible unit integer customers' perceived value of water transportation for OD pairs, indexed by b.

M A sufficiently large positive number.

Newly defined variables:

λ_{pb}^W binary, equals one if unit integer customers' perceived value of water transportation for OD pair p is b, and otherwise zero, which is related with γ_p^W.

ξ_p^{LW} continuous, land transportation volume of OD pair p when unit customers' perceived value of water transportation for OD pair p is γ_p^W, equal to the product of the variable η_p^L and the variable γ_p^W.

ξ_p^{WW} continuous, equal to the product of the variable η_p^W and the variable γ_p^W.

μ_{ygd} continuous, route plan y's transportation volume via water when leg $g \in G_y$' transportation is under policy degree d, $\mu_{ygd} \in [0, \bar{n}_p]$.

φ_a binary, equals one if area a is used and otherwise zero.

Newly defined constraints:

$$\xi_p^{WW} + \xi_p^{LW} = \bar{n}_p \cdot \gamma_p^W \qquad \forall p \in P \qquad (4\text{-}13)$$

$$v_p^L \cdot \eta_p^W = \xi_p^{LW} \qquad \forall p \in P \qquad (4\text{-}14)$$

$$\mu_{ygd} \le \bar{n}_p \cdot \theta_{gd} \qquad \forall p \in P, y \in Y_p, g \in G_y, d \in D \qquad (4\text{-}15)$$

$$\mu_{ygd} \le \pi_y \qquad \forall p \in P, y \in Y_p, g \in G_y, d \in D \qquad (4\text{-}16)$$

$$\mu_{ygd} \ge \pi_y - \bar{n}_p(1 - \theta_{gd}) \qquad \forall p \in P, y \in Y_p, g \in G_y, d \in D \qquad (4\text{-}17)$$

$$\xi_p^{WW} = \sum_{y \in Y_p} \left(\sum_{g \in G_y} \sum_{d \in D} v_{gd}^W \mu_{ygd} - \pi_y v_y^{-T} \right) \qquad \forall p \in P \qquad (4\text{-}18)$$

$$\sum_{b \in B} b \lambda_{pb}^W \le \gamma_p^W \qquad \forall p \in P \qquad (4\text{-}19)$$

$$\gamma_p^W \le \sum_{b \in B} (b+1) \lambda_{pb}^W \qquad \forall p \in P \qquad (4\text{-}20)$$

$$\sum_{b \in B} \lambda_{pb}^W = 1 \qquad \forall p \in P \qquad (4\text{-}21)$$

$$\xi_p^{WW} \le (b+1)\eta_p^W + B(1 - \lambda_{pb}^W) \qquad \forall p \in P, b \in B \qquad (4\text{-}22)$$

$$\xi_p^{WW} \ge b\eta_p^W - B(1 - \lambda_{pb}^W) \qquad \forall p \in P, b \in B \qquad (4\text{-}23)$$

$$\sum_{d \in D} d\beta_{ad} \le \sum_{d \in D} d\theta_{gd} \qquad \forall g \in G, a \in A_g \qquad (4\text{-}24)$$

$$\sum_{d \in D} d\beta_{ad} \ge \sum_{d \in D} d\theta_{gd} - M(1 - \varphi_a) \qquad \forall g \in G, a \in A_g \qquad (4\text{-}25)$$

$$\sum_{a \in A_g} \varphi_a \ge 1 \qquad \forall g \in G \qquad (4\text{-}26)$$

$$\mu_{ygd} \in [0, \bar{n}_p] \qquad \forall p \in P, y \in Y_p, g \in G_y, d \in D \qquad (4\text{-}27)$$

$$\xi_p^{WW}, \xi_p^{LW} \in \mathbb{R} \qquad \forall p \in P \qquad (4\text{-}28)$$

$$\lambda_{pb}^W \in \{0,1\} \qquad \forall p \in P, b \in B \qquad (4\text{-}29)$$

$$\varphi_a \in \{0,1\} \qquad \forall g \in G, a \in A_g \qquad (4\text{-}30)$$

After applying the above linearization methods, model [M1] is rewritten as:

[**M2**] Minimize $\sum_{p \in P} \left[\dot{e}_p^L \eta_p^L + \sum_{y \in Y_p} \sum_{g \in G_y} \sum_{d \in D} \dot{e}_{gd}^W \mu_{ygd} \right]$ (4-31)

subject to (4-2)-(4-6), (4-9)-(4-30).

5. Exact solution algorithm

For large-scale problems, some commercial solvers cannot solve model M2 in a reasonable time. The reason for this may be that linearization dramatically increases the difficulty of solving model M2.

In addition, when the number of regions is large, the number of policy assignment plans for different areas (i.e., $|D^A|$) also becomes very large, which makes the solving process even more time consuming. Thus, this section proposes a tailored solution algorithm to solve model M2 efficiently. The algorithm is based on branch and bound and mainly branches the variable β_{ad}, which is a key variable in this model. If we fix β_{ad} in the model, θ_{gd} is determined and Constraints (4-15)–(4-17) are no longer needed. This dramatically reduces the size of the model and the difficulty of the solution. Therefore, we develop a tailored branch-and-bound algorithm to solve the model.

We first introduce a node (subproblem) branching strategy used in the tailored branch-and-bound algorithm that branches β_{ad} to lighten the computation burden in Section 5.1. Then, in Section 5.2, we formulate a linear submodel of the original model M2 under a given policy assignment plan (a group of β_{ad} values). This submodel can be efficiently solved using CPLEX. Furthermore, we derive some propositions based on the properties of model M1 to accelerate the algorithmic solving process. Finally, we present a detailed description of the tailored branch-and-bound algorithm in Section 5.3.

5.1 Branching scheme

In the model, the core decision variables are to decide the policy for the degree of emission control in all areas of the water region (i.e., β_{ad}). Once the values of β_{ad} are determined, the split of cargo transportation volume between land and water can be solved, and the total emissions of both land transportation and water transportation are thus obtained. Thus, in the algorithm, we branch on β_{ad}. As an area a can only be assigned to one emission control policy, the solution space can be partitioned using a policy assignment variable space. Regarding one area, once an emission control policy is selected, the remaining policy of the corresponding area can be eliminated from consideration. A group of β_{ad} values that satisfy Constraint (4-2) is called a policy assignment plan. Therefore, our partitioning divides the policy assignment space into $|D^A|$ subspaces. The cargo splitting problem between land and water (the subproblem) is separated from the original problem at each branch by fixing β_{ad}. An example with $|A| = 3$ and $|D| = 2$ is shown in Figure 3 to illustrate the branching scheme of the algorithm.

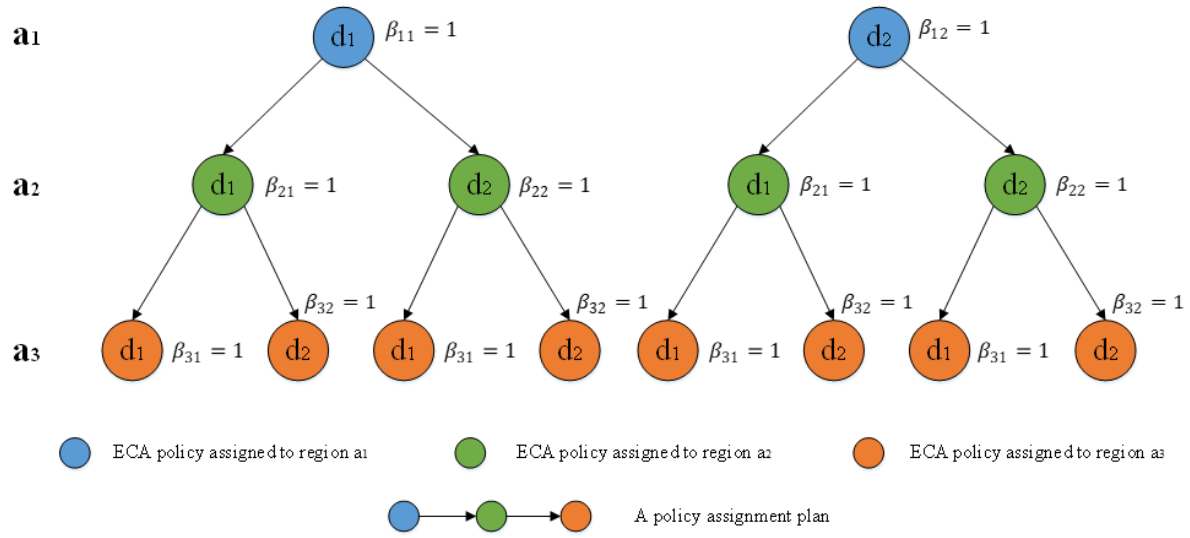

Figure 3: Illustration of the branching scheme of the branch-and-bound algorithm

To constitute a policy assignment plan, areas are sorted in decreasing order of the number of times each area is passed by legs. For the example in Figure 3, a_1 represents the area that has been passed by the legs the most times, a_2 represents the area that has been passed by the legs the second most times, and a_3 represents the area passed by the legs the least number of times. d_1 denotes the policy with the highest degree of emission control, and d_2 denotes the policy with the lowest degree of emission control. Initially, a_1 is selected and is first assigned to policy d_1. Next, a_2 is assigned to policy d_1, and then likewise a_3. A policy assignment plan is thus determined. For each area a, only one policy assignment variable equals one and the remaining variables are set to zero. For the example in Figure 3, we assume that there are two available emission control policies d_1 and d_2 for a selected area a_1. Two subnodes are then associated with the following tuples: $\{\beta_{11} = 1,\ \beta_{12} = 0\}$, $\{\beta_{11} = 0,\ \beta_{12} = 1\}$, respectively. In Figure 3, the three different colored circles represent the policy assigned to different areas, which together form a completely policy assignment plan. For example, the leftmost combination of circles expresses a plan with the values of $\{\beta_{11} = 1,\ \beta_{21} = 1,\ \beta_{31} = 1\}$. As shown in Figure 3, branching in this algorithm is executed from bottom to top, left to right. From the analysis of the problem structure, we observe the following proposition:

Proposition 1: For the area with the least number of leg passes, a stricter emission policy (a smaller sulfur cap) leads to a higher or unchanged total sulfur emission.

Proof: See Appendix A. ■

Proposition 1 is used in the branching scheme that decreases the policy assignment space into $|D^{A-1}|$, and the detailed description of the branching scheme is as follows. Through the branching procedure, the output is the objective value represented by UB, which is also the optimal solution.

Branching scheme

1: Define $\widetilde{\mathrm{A}}$ as the set of areas, $\widetilde{\mathrm{A}} = \{a_1, \cdots, a_i\}$, where areas are sorted according to the decreasing order of the times for which they are passed by legs. Define $\widetilde{\mathrm{D}}$ as the set of emission control policies, $\widetilde{\mathrm{D}} = \{d_1, \cdots, d_j\}$, where policies are sorted according to the decreasing order of the sulfur cap. Set the Upper Bound $UB = +\infty$.
2: *for* $d_j \in \widetilde{\mathrm{D}}$ assigned to a_1
3: *for* $d_j \in \widetilde{\mathrm{D}}$ assigned to a_2
4: ⋮
5: *for* $d_j \in \widetilde{\mathrm{D}}$ assigned to a_i
6: Solve the subproblem by CPLEX and obtain the current objective value OBJ_{cur}
7: **if** $OBJ_{cur} > UB$ **then**
8: **break**;
9: **else if** $OBJ_{cur} \leq UB$ **then**
10: $UB = OBJ_{cur}$;
11: **continue**;
12: *end for*
13: ⋮
14: *end for*
15: *end for*

5.2 Subproblem under a given policy assignment plan

Given a policy assignment plan, the algorithm solves a cargo splitting problem for land and water transportation ways. When β_{ad} is determined, values of θ_{gd} variable could be determined accordingly. The degree of emission control policy that a voyage leg must obey should be the highest emission control degree of the multiple areas that the leg crosses. In addition, given value of θ_{gd}, Constraints (4-15)~(4-17) are no longer required, which largely reduces the computational difficulty. Besides, Constraints (4-2)~(4-4) and (4-24)~(4-26) are also not needed due to the fixed β_{ad}. In the subproblem model, $\bar{\theta}_{gd}$ is regarded as a parameter and then Constraints (4-18) can be rewritten as Constraints (5-2). Thus, the subproblem can be efficiently solved by the CPLEX. The subproblem model under a given policy assignment plan is represented as M2_sub, shown as follows.

[**M2_sub**] *Minimize* $\sum_{p\in P}\left[\dot{e}_p^L \eta_p^L + \sum_{y\in Y_p} \pi_y \left(\sum_{g\in G_y}\sum_{d\in D} \dot{e}_{gd}^W \bar{\theta}_{gd}\right)\right]$ (5-1)

subject to: Constraints (4-5)~(4-6), (4-11)~(4-14), (4-19)~(4-23), (4-28)~(4-30), and

$$\xi_p^{WW} = \sum_{y\in Y_p} \pi_y \left(\sum_{g\in G_y}\sum_{d\in D} v_{gd}^W \bar{\theta}_{gd} - v_y^{-T}\right) \qquad \forall p \in P \tag{5-2}$$

In this subproblem, the most essential decision is the β_{ad} variable, i.e., the degree of emission control policy in each area. The following proposition states that when the core decision β_{ad} is determined, which also implies θ_{gd} variable is determined, there may exist a closed form formula on calculating the objective value and the other decision variables' values, under some conditions.

Proposition 2: Given the values of the variables θ_{gd}, if $\max_{y\in Y_p}\left\{\sum_{g\in G_y}\sum_{d\in D}\dot{e}_{gd}^{W}\theta_{gd}\right\} < \dot{e}_p^L$, M1's objective value is: $\bar{n}_p\dot{e}_p^L - \frac{\bar{n}_p \max_{y\in Y_p}\left\{\sum_{g\in G_y}\sum_{d\in D}v_{gd}^{W}\theta_{gd}-v_y^{-T}\right\}}{\max_{y\in Y_p}\left\{\sum_{g\in G_y}\sum_{d\in D}v_{gd}^{W}\theta_{gd}-v_y^{-T}\right\}+v_p^L}\left(\dot{e}_p^L - \sum_{g\in G_y: y=\operatorname{argmax}_{y\in Y_p} v_y^W}\sum_{d\in D}\dot{e}_{gd}^{W}\theta_{gd}\right)$. The values of decision variable are: $\pi_y = \eta_p^W$ for $y = \operatorname{argmax}_{y\in Y_p}\left\{\sum_{g\in G_y}\sum_{d\in D}v_{gd}^{W}\theta_{gd} - v_y^{-T}\right\}$ and $\pi_y = 0$ for $y \in Y_p \setminus \left\{\operatorname{argmax}_{y\in Y_p}\left\{\sum_{g\in G_y}\sum_{d\in D}v_{gd}^{W}\theta_{gd} - v_y^{-T}\right\}\right\}$.

Proof: See Appendix A. ■

In the above proposition, the condition $\max_{y\in Y_p}\left\{\sum_{g\in G_y}\sum_{d\in D}\dot{e}_{gd}^{W}\theta_{gd}\right\} < \dot{e}_p^L$ means that the largest emission of a route plan among all the route plans for an OD pair p is less than the emission of the land transportation for the OD pair. This condition actually holds in reality. Therefore, this proposition is potentially meaningful for practical applications. The closed form of the objective value could be used to evaluate the lower bound value of one certain $\boldsymbol{\beta}$-featured solution.

Although the above condition holds in the reality with respect to some criteria such as sulfur emission, the contrary of that condition may exist, i.e., $\min_{y\in Y_p}\left\{\sum_{g\in G_y}\sum_{d\in D}\dot{e}_{gd}^{W}\theta_{gd}\right\} > \dot{e}_p^L$, which means that the least emission of a route plan among all the route plans for an OD pair p is greater than the emission of the land transportation for the OD pair. For this case, another proposition is proved as follows.

Proposition 3: Given the values of the variables θ_{gd}, if $\min_{y\in Y_p}\left\{\sum_{g\in G_y}\sum_{d\in D}\dot{e}_{gd}^{W}\theta_{gd}\right\} > \dot{e}_p^L$, M1's objective value is: $\bar{n}_p\dot{e}_p^L - \frac{\bar{n}_p \min_{y\in Y_p}\left\{\sum_{g\in G_y}\sum_{d\in D}v_{gd}^{W}\theta_{gd}-v_y^{-T}\right\}}{\min_{y\in Y_p}\left\{\sum_{g\in G_y}\sum_{d\in D}v_{gd}^{W}\theta_{gd}-v_y^{-T}\right\}+v_p^L}\left(\dot{e}_p^L - \sum_{g\in G_y: y=\operatorname{argmin}_{y\in Y_p} v_y^W}\sum_{d\in D}\dot{e}_{gd}^{W}\theta_{gd}\right)$. The values of decision variable are: $\pi_y = \eta_p^W$ for $y = \operatorname{argmin}_{y\in Y_p}\left\{\sum_{g\in G_y}\sum_{d\in D}v_{gd}^{W}\theta_{gd} - v_y^{-T}\right\}$ and $\pi_y = 0$ for $y \in Y_p \setminus \left\{\operatorname{argmin}_{y\in Y_p}\left\{\sum_{g\in G_y}\sum_{d\in D}v_{gd}^{W}\theta_{gd} - v_y^{-T}\right\}\right\}$.

Proof: See Appendix B. ■

In either Proposition 2 or Proposition 3, it is important to calculate the largest emission ($\max_{y\in Y_p}\left\{\sum_{g\in G_y}\sum_{d\in D}\dot{e}_{gd}^{W}\theta_{gd}\right\}$) or the least emission ($\min_{y\in Y_p}\left\{\sum_{g\in G_y}\sum_{d\in D}\dot{e}_{gd}^{W}\theta_{gd}\right\}$) for each OD pair when

value of $\boldsymbol{\theta}$ variable is given; it is also important to determine the route plan with the largest customers' perceived value ($\underset{y\in Y_p}{\operatorname{argmax}}\left\{\sum_{g\in G_y}\sum_{d\in D} v_{gd}^{W}\theta_{gd} - v_y^{-T}\right\}$) or the route plan with the least customers' perceived value ($\underset{y\in Y_p}{\operatorname{argmin}}\left\{\sum_{g\in G_y}\sum_{d\in D} v_{gd}^{W}\theta_{gd} - v_y^{-T}\right\}$).

Although Figure 2 just demonstrates four route plans for the OD pair between Port 2 and Port 9. From theoretical perspective, the number of possible route plans for the OD pair may be not trivial. For an OD pair that contains n ports between the origin and the destination ports, the size of the set Y_p, i.e., $|Y_p|$ equals to $C_n^0 + C_n^1 + \cdots + C_n^n = n!$. Therefore, it may be time consuming to enumerate all the route plans in a large set Y_p so as to calculate the above values mentioned in the previous paragraph. Some propositions are proved as follows so as to facilitate the process of determining the above-mentioned values.

Proposition 4: Given the values of the variables θ_{gd}, for each OD pair p, the maximum and minimum emission of a route plan is calculated as follows:

$\min_{y\in Y_p}\left\{\sum_{g\in G_y}\sum_{d\in D}\dot{e}_{gd}^{W}\theta_{gd}\right\} = \dot{e}_{gd}^{W}$, where g is the longest leg for the OD pair p, and d is the highest degree among all the emission control degrees of areas that this leg covers.

$\operatorname{Max}_{y\in Y_p}\left\{\sum_{g\in G_y}\sum_{d\in D}\dot{e}_{gd}^{W}\theta_{gd}\right\} = \sum_{g\in \bar{G}_p}\sum_{d\in D}\dot{e}_{gd}^{W}\theta_{gd}$, where $\bar{G}_p$ is the set of legs that constitute the OD pair p, and each leg is included in one and only one area.

Proof: See Appendix C. ■

Through the Proposition 4, the important part $\max_{y\in Y_p}\left\{\sum_{g\in G_y}\sum_{d\in D}\dot{e}_{gd}^{W}\theta_{gd}\right\}$ and $\min_{y\in Y_p}\left\{\sum_{g\in G_y}\sum_{d\in D}\dot{e}_{gd}^{W}\theta_{gd}\right\}$ for each OD pair p used in the Propositions 2 and 3 can be determined immediately.

The minimum total emission can be calculated as follows. For each OD pair p, there exists three cases: (i) when $\max_{y\in Y_p}\left\{\sum_{g\in G_y}\sum_{d\in D}\dot{e}_{gd}^{W}\theta_{gd}\right\} < \dot{e}_p^{L}$, the sulfur emission can be obtained by the Proposition 2. (ii) when $\min_{y\in Y_p}\left\{\sum_{g\in G_y}\sum_{d\in D}\dot{e}_{gd}^{W}\theta_{gd}\right\} > \dot{e}_p^{L}$, the sulfur emission can be obtained by the Proposition 3. (iii) when $\min_{y\in Y_p}\left\{\sum_{g\in G_y}\sum_{d\in D}\dot{e}_{gd}^{W}\theta_{gd}\right\} \le \dot{e}_p^{L} \le \max_{y\in Y_p}\left\{\sum_{g\in G_y}\sum_{d\in D}\dot{e}_{gd}^{W}\theta_{gd}\right\}$, we assume the total volume of transportation demand for OD pair p are satisfied by water transportation, so as to get the minimum sulfur emission of OD pair p. Thereby, under a given policy assignment plan, the minimum total sulfur emission is obtained and can be set as the lower bound. The lower bound can be

used to determine whether the following subproblem needs to be solved, and the solution can be obtained by the proposed algorithm in a shorter time. Firstly, the objective value of the first policy assignment plan needs to be solved, which can be set as the optimal solution sol_opt. For the next policy assignment plan, we first compute the lower bound. The objective function of the model aims to minimize sulfur emission. Thus, if the lower bound is larger than sol_opt, there is no need to continue the calculation of the subsequent subproblem by CPLEX. If the lower bound is smaller than sol_opt, then the subproblem is solved by CPLEX.

5.3 A tailored branch-and-bound algorithm

The detailed description of the B&B algorithm for solving model M2 is summarized as follows:

Algorithm 1. Tailored branch-and-bound algorithm

Step 0. (*Initialization*) Define K as the set of all policy assignment plans. Set the optimal objective value Obj_opt $= \infty$.

Step 1. (*Initial solution*) Set the incumbent subproblem M2_sub with first policy assignment plan k $= 1$. Obtain the initial objective value Obj_ini. Set $Obj_{opt} \leftarrow Obj\_ini$.

Step 2. (*Problem branching*) Refer to the strategy shown in Section 5.1.

Step 3. (*Subproblem solution*) For each $k \in K$, solve each subproblem descripted in Section 5.2. Obtain the current objective value Obj_{cur}.

Step 4. (*Branch fathoming*) For each $k \in K$, if Obj_{cur} < UB, then continue to branch; else, stop branching. If $Obj_{cur} < Obj_{opt}$, then set $Obj_{opt} \leftarrow Obj_{cur}$.

Step 5. (*Output optimal solution*) Obtain the optimal plan k^* with the optimal objective value Obj_{opt}.

6. Numerical experiments

6.1 Performance of the algorithm

Before using the proposed model and algorithm for numerical experiments, we need to validate the performance of the proposed algorithm. To do this, we apply the tailored branch-and-bound algorithm to solve model M2 in some small-scale scenarios. To verify the algorithm, we carry out a number of numerical experiments over scenarios with different numbers of OD pairs. In these scenarios, the values of d_g^W and d_p^L are randomly generated between [20,250] (nm) and [100,600] (km), and the total volume of transportation for OD pair p is randomly generated between 500 and 2000 tons. We compare the results obtained by the proposed tailored branch-and-bound algorithm with those obtained by the enumeration algorithm. Each policy assignment plan with the variable β_{ad} is enumerated in the enumeration algorithm, which means the problem size is $|D^A|$. The performance of the algorithms is

measured in terms of CPU time using the two methods. Table 1 compares the two algorithms. We can see that although the objective values obtained by the two algorithms are identical, the solution time using the enumeration algorithm is much longer than that using the tailored algorithm.

Table 1: Algorithmic performance of the tailored branch-and-bound algorithm

Instances	The tailored branch and bound algorithm		The enumeration algorithm	
ID	Obj	CPU time (s)	Obj	CPU time (s)
5-1	4344.12	34	4344.12	43
5-2	2264.62	99	2264.62	124
5-3	3279.43	58	3279.43	76
5-4	2097.89	78	2097.89	91
5-5	4352.07	48	4352.07	55
10-1	6444.98	200	6444.98	304
10-2	4266.72	117	4266.72	269
10-3	7111.29	266	7111.29	343
10-4	4331.70	119	4331.70	251
10-5	5667.82	246	5667.82	335
20-1	13277.01	1421	13277.01	1693
20-2	14837.50	923	14837.50	1346
20-3	15715.53	793	15715.53	1282
20-4	11273.44	1038	11273.44	1475
20-5	14211.35	1280	14211.35	1821

Notes: Instance ID "5-#" means that there are 5 OD pairs in the instance; '#' is the index of the instances.

6.2 Performance of the proposed model

We apply the proposed algorithm to optimize the emission control policy for two inland river shipping networks in China. The demand for OD pairs is estimated using port throughput data in 2023. The experimental setting is as follows. Suppose that the travel distance via land transportation for OD pair p is denoted by d_p^L, and the unit emission coefficient via land transportation is u^L (g/ton·km), which is estimated at 0.17 (Hoen et al., 2014). Consequently, the parameter $\dot{e}_p^L$ (g/ton) is equal to 0.17 multiplied by d_p^L. Suppose that u_d^W is the unit emission coefficient via water transportation under policy degree d (g/ton·km) and d_g^W is the travel distance via water transportation for leg $g \in G_y$, with $y \in Y_p$. The values of u_d^W with policy degrees of 0.05%, 0.1%, and 0.5% for fuel sulfur limits are set to 0.004, 0.01, and 0.05, respectively (Gang & Lee, 2020; Zhen et al., 2020). The travel distance data related to land and water transportation are obtained from a professional geographical database.

The parameter $\dot{e}_{gd}^{W}$, i.e., the unit emission via water transportation for leg g under policy degree d, is calculated as $u_d^W \times d_g^W$. Customers' perceived value is defined as a weighted sum of the reciprocal of the delivery time and the reciprocal of the delivery cost. Here we suppose that the weights for the time and cost of land and water transportation are denoted by h_c^L, h_t^L, h_c^W, and h_t^W, which are set to 0.3, 0.7, 0.7, and 0.3, respectively (Fan et al., 2019). Other parameters used to calibrate customers' perceived value are defined as follows:

$\overline{c}_d^W$ unit cost of low sulfur fuel oil per travel distance under policy degree d.

$\overline{c}^L$ unit cost of fuel oil per travel distance via land transportation.

$\overline{v}^L$ truck average speed via land transportation.

$\overline{v}^W$ ship speed using the most economical mode of travel.

The previously defined parameters v_p^L and v_{gd}^W can then be calculated as $v_p^L = h_t^L \overline{v}^L / d_p^L + h_c^L / (d_p^L \overline{c}^L)$ and $v_{gd}^W = h_t^W \overline{v}^W / d_g^W + h_c^W / (d_g^W \overline{c}_d^W)$, respectively. The unit of customers' perceived value of water transportation is based on the shortest path of the leg. Based on current fuel prices, we set the unit cost of fuel oil with 0.05% sulfur content, 0.1% sulfur content, and 0.5% sulfur content to 28.7 (¥/km), 17.3 (¥/km), and 10.8 (¥/km), respectively (Ship & Bunker, 2023), while the unit cost of fuel oil via land transportation is set to 30 (¥/km). Moreover, we set the values of $\overline{v}^L$ and $\overline{v}^W$ to 40 km/h and 15 knots, respectively (Palak et al., 2014). All of our experiments are coded in C# (Visual Studio 2019) and run on a computer with a 2.1GHz Intel Core i7 and 32 GB of RAM.

The first case study is conducted for the Yangtze River. The experiment is based on a shipping network that consists of seven ports distributed on the Yangtze River, as shown in Figure 4. In this study, the division of areas is based on provincial boundaries. Specifically, these seven ports are distributed across four provinces, so the river region in this case is divided into four areas—Jiangsu province, Anhui province, Jiangxi province, and Hubei province. The degree of emission control is considered to be the percentage of sulfur content permitted in bunker fuel. Here, three alternative sulfur content limits for fuel are taken into account: 0.5%, 0.1%, and 0.05%. Seven ship routes and 16 OD pairs are considered in this case. The optimal emission control policy (i.e., the sulfur cap) in each area is reported in Table 2. The total sulfur emissions from sea and land transportation amount to 415.81 kilograms. Under the current emission control policy in this inland river, which is implemented with a homogenous setting of a 0.1% sulfur limit, the total emission is 417.08 kilograms, resulting in an emission reduction of 1.27 kilograms.

Figure 4: A shipping network on the Yangtze river

Table 2: Results of heterogeneous settings on sulfur limits for Yangtze River areas

River area	Jiangsu	Anhui	Jiangxi	Hubei	Total emission (kg)
Sulfur cap	0.1	0.5	0.1	0.1	415.81

Another case focuses on the Pearl River basin. Six representative ports along the Pearl River are selected to construct a small shipping network, as shown in Figure 5. This network has five ship routes. In this case, the Pearl River is divided into three areas—Guizhou province, Guangxi province, and Guangdong province. Table 3 illustrates the optimal emission control policy (i.e., the sulfur cap) for the Pearl River. With a heterogeneous sulfur limit setting, the total emission is 303.17 kilograms. In the context of the current inland river emission control policy, the total sulfur emissions of sea and land transportation are 304.61 kilograms. The heterogeneous emission control policy can thus reduce emissions by about 1.44 kilograms compared with the homogeneous policy. These two cases validate the improved performance of the proposed heterogeneous emission control policy in each area along an inland river.

Figure 5: A shipping network on the Pearl River

Table 3: Results of heterogeneous settings on sulfur limits for Pearl River areas

River area	Guangdong	Guangxi	Guizhou	Total emission (kg)
Sulfur cap	0.1	0.5	0.05	303.17

From Table 2 and Table 3, we can see that Anhui and Guangxi provinces have much looser emission control policy than other areas. The reason is that most of the legs related to ports in Anhui/ Guangxi Province are connected to ports in other provinces, which means that these legs include multiple areas. For instance, leg related to Anhui (i.e. Wuhu-Nanjing) and leg related to Guangxi (i.e. Wuzhou-Guangzhou) both pass through two areas. According to the rules in this paper (constraints (4-4)), a ship on a given voyage must obey the strictest emission control policy across multiple areas. Consequently, the policy impact of Anhui and Guangxi Provinces is relatively small and loose.

Moreover, based on the comparison with the current homogeneous policy, we can see the current homogeneous policy is also effective in reducing emissions, although it is relatively simple and single. The heterogeneous policy is not necessary as its relatively complex considerations. However, the OD pairs considered in the current case are not large in scale. And as the transportation demand scales up, the emission reduction can be more significant. We further calculate the situation that the entire areas in inland river are taken the strictest emission policy of a 0.05% sulfur limit, in which the total emission is 456.18 and 336.47 kilograms respectively in two cases. The results show that under this situation there is a remarkable increase in the total sulfur emission compared to the homogenous setting of a 0.1% sulfur limit. This indicates that stricter policies do not necessarily result in lower sulfur emissions.

6.3 Sensitivity analysis

In reality, the price of marine fuel fluctuates and may influence emissions. The first series of sensitivity analyses is conducted to investigate the impact on emissions of the unit cost of fuel with a

sulfur content of 0.05%. Specifically, we use the previously mentioned Pearl River case as the benchmark case, and the unit cost of fuel oil is denoted by $\overline{c}_{0.05}^{W}$. We design six cases: Cases 1, 2, and 3 mean that $\overline{c}_{0.05}^{W}$ decreases by 10%, 20%, and 30%, respectively; Cases 4, 5, and 6 mean that $\overline{c}_{0.05}^{W}$ increases by 10%, 20%, and 30%, respectively. Suppose that Obj_0 is the sulfur emissions of the benchmark case and Obj_x is the sulfur emissions of Case x. The gap is calculated as $(Obj_x - Obj_0)/Obj_0$. For Cases 1–6, the results of the gap value and the optimal sulfur caps in different areas are shown in Table 4.

Table 4: Results under different unit costs of fuel with 0.05% sulfur content

River area	Case 1	Case 2	Case 3	Case 4	Case 5	Case 6
Guangdong	0.1	0.1	0.5	0.5	0.5	0.5
Guangxi	0.5	0.5	0.1	0.1	0.1	0.1
Hubei	0.05	0.05	0.05	0.1	0.1	0.1
Gap (%)	-0.40	-0.94	-1.65	0.04	0.04	0.04

The trend observed in Table 4 shows that, in general, the sulfur emissions decrease with a decrease in $\overline{c}_{0.05}^{W}$. Moreover, the optimal sulfur caps remain unchanged in case 1 and case 2, and changes in Case 3. This result is as expected because as the unit cost of fuel with a sulfur content of 0.05% decreases, which means the price difference among $\overline{c}_{0.05}^{W}$, $\overline{c}_{0.1}^{W}$ and $\overline{c}_{0.5}^{W}$ gets smaller, it becomes more preferable to choose looser sulfur cap. The optimal sulfur cap variation leads to an increase in the volume via water transportation, thereby the total sulfur emission is reduced. However, the sulfur emission gap and optimal sulfur cap are consistent in Cases 4, 5, and 6. The reason is that the unit cost of fuel with a sulfur content of 0.05% have already pretty higher than the unit cost of fuel with a sulfur content of 0.1% and 0.5%. Consequently, the increase in $\overline{c}_{0.05}^{W}$ has little impact on sulfur emissions.

A sensitivity analysis is also conducted for the unit cost of fuel oil with 0.1% sulfur content ($\overline{c}_{0.1}^{W}$). For Cases 7, 8, and 9, $\overline{c}_{0.1}^{W}$ decreases by 10%, 20%, and 30%, respectively; and for Cases 10, 11, and 12, $\overline{c}_{0.1}^{W}$ increases by 10%, 20%, and 30%, respectively. The results are shown in Table 5. The gap between Cases 7–9 and Case 0 decreases sharply as $\overline{c}_{0.1}^{W}$ decreases. This indicates that a reduction in the unit cost of fuel oil with 0.1% sulfur content has a significant impact on sulfur emissions. The reason is that the lower the unit cost of fuel oil, the higher the customers' perceived value of water transportation, and the lower the sulfur emissions per unit. The sulfur emission gap between Case 10 (11 or 12) and Case 0 changes slightly as $\overline{c}_{0.1}^{W}$ increases. However, the gap value remains unchanged in the context of an increase in $\overline{c}_{0.05}^{W}$.

Table 5: Results under different unit costs of fuel with 0.1% sulfur content

River area	Case 7	Case 8	Case 9	Case 10	Case 11	Case 12
Guangdong	0.1	0.1	0.1	0.1	0.5	0.5
Guangxi	0.1	0.1	0.1	0.5	0.5	0.5
Hubei	0.1	0.1	0.1	0.05	0.05	0.05
Gap (%)	-2.90	-7.09	-11.64	1.47	1.66	1.66

A similar sensitivity analysis is also conducted for fuel oil with 0.5% sulfur content. The unit cost of fuel oil is denoted by $\overline{c}_{0.5}^{W}$. In Cases 13, 14, and 15, $\overline{c}_{0.5}^{W}$ decreases by 10%, 20%, and 30%, respectively; while in Cases 16, 17, and 18, $\overline{c}_{0.5}^{W}$ increases by 10%, 20%, and 30%, respectively. The results, summarized in Table 6, are similar to those in the previous two tables.

Table 6: Results under different unit costs of fuel with 0.5% sulfur content

River area	Case 13	Case 14	Case 15	Case 16	Case 17	Case 18
Guangdong	0.5	0.5	0.5	0.1	0.1	0.1
Guangxi	0.5	0.5	0.5	0.1	0.1	0.1
Hubei	0.05	0.05	0.05	0.1	0.1	0.1
Gap (%)	-1.52	-5.20	-9.01	0.48	0.48	0.48

We also analyze the influence of the average speed via land transportation, $\overline{v}^{L}$, and water transportation, $\overline{v}^{W}$. Two series of sensitivity analyses on the average speed are performed: (i) we fix the ship speed via water transportation at 15 knots and vary the truck speed using a set of six values—30, 40, 50, 60, 70, and 80 km/h; and (ii) we maintain the truck speed at 40km/h and vary the ship speed using a set of six values—13, 14, 15, 16, 17, and 18 knots. The results in Figure 6(a) imply that the sulfur emission gap increases as truck speed increases. The reason for this is that the higher the truck speed, the higher the customers' perceived value via land transportation. Transportation demand is then more fulfilled by land transportation, and total sulfur emissions thus increase due to higher unit emission via land transportation relative to water transportation. From figure 6(b), we can see that when the ship speed is larger than 15 knots, the emission gap is less than 0 and is getting bigger, whereas the gap is more than 0 when the ship speed is smaller than 15 knots. This is because the impact of ship speed is twofold. It has an effect not only on the sailing time, but also on the fuel consumption, which is related to sulfur emission. Thus, the increase in speed will increase emissions while decreasing travel time.

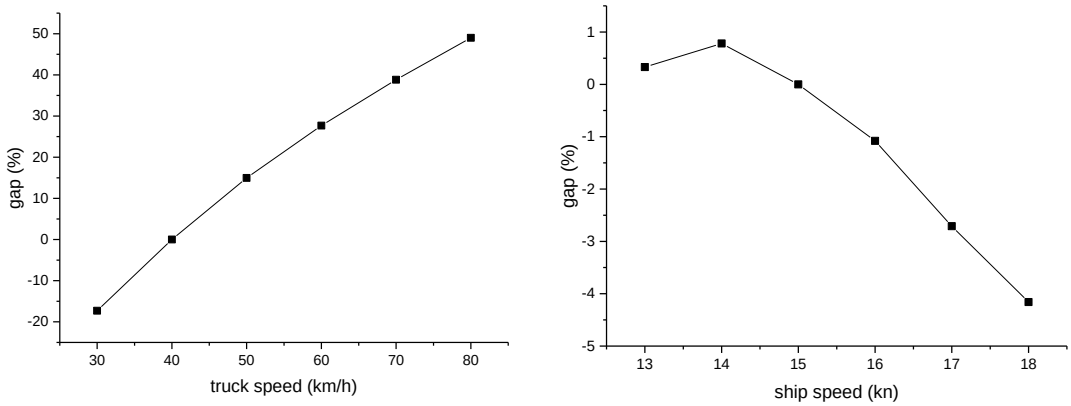

(a) (b)

Figure 6: Sensitivity of sulfur emission gaps to truck speed and ship speed

Based on the results obtained in the numerical experiments, it is suggested for government to consider the heterogeneous setting on sulfur limits in distinct areas along the inland river, which potentially reduce total emissions further compared to current homogenous sulfur limit policy from a theoretical perspective. We find that strict emission policies in inland river may lead to a shift in transportation demand from water to land, affecting overall emissions. Thus, it is recommended to take the situation of land transportation into account when formulating emission policies for waterway. In addition, fuel prices with different sulfur contents and sailing speed of the ships are also important factors influencing the sulfur emission.

7. Conclusions

This paper conducts an explorative study on emission control policymaking to achieve sustainable river shipping transportation. An MILP model is formulated for ECA design considering heterogeneous sulfur caps in distinct areas along a river. A branch-and-bound algorithm is also developed to solve the proposed model efficiently. The main contributions of this study can be summarized in the following three aspects.

First, this paper may be the first to apply mathematical programming to emission control policymaking for river transportation. The novelty of the proposed model lies in its consideration of heterogeneous sulfur caps along a river. This can be potentially useful for further reducing the total combined emissions from land transportation and water transportation compared with the traditional homogenous policy of emission control.

Second, different from studies on emission control for shipping, the aim of our proposed model is to minimize the total combined emissions from land transportation and water transportation rather than to focus only on ship emissions. Thus, the proposed methodology in this study may be more suitable for

improving social benefits and sustainability instead of being limited solely to the water transportation industry.

Finally, the methodology (i.e., the model and the algorithm) designed in this study can serve as a decision support tool for policymaking for water transportation. The deliverable of this study is that it can help make the policymaking process, which is usually based on decision makers' experience and implicit knowledge, more rational and scientific.

This study also has limitations. For example, although it is oriented toward policymaking related to water transportation, the methodology cannot be directly applied to maritime transportation, which accounts for the majority of the water transportation sector by transportation volume. However, to determine the emission control policy usually is a complex process, governments often base their decisions on a broader range of factors. In reality, the geographical location of the port is closely related to transportation demands. For example, Suzhou Port is located in the throat of the Yangtze River estuary, and is also in the Yangtze River Delta Economic Zone, with a high population density, and thus has relatively high demand. To improve the practicality, the local economic level of the port and its position in the overall river (upstream, downstream) can be taken into account when considering differences in demand. In the future, the studied model could be further extended and improved, by considering uncertainty demand related to population density and geographic conditions. Additionally, ships would burn different sulfur content fuels for compliance with ECA to save sailing costs in offshore and deep-sea shipping. The potential increase in the fuel switching time may affect the demand split. Hence, some modifications integrated fuel switching strategy in the model can be another direction for future research. In addition, when solving large-scale problems, some heuristics like ALNS algorithm can be considered to further improve speed.

Acknowledgements

This research is supported by the National Natural Science Foundation of China (Grant numbers 71831008, 72025103, 72361137001, 72201163, 72071173, 72371221, 72361137006) and the Research Grants Council of the Hong Kong Special Administrative Region, China [Project number HKSAR RGC TRS T32-707/22-N].

Appendices

Appendix A: Proof of Proposition 1

Proposition 1: For the area with the least number of leg passes, a stricter emission policy (a smaller sulfur cap) leads to a higher or unchanged total sulfur emission.

Proof: For the area with the least number of leg passes, focusing on the situation when a stricter emission policy is implemented in this area, there are two cases as follows: (i) It will not affect the policy obeyed by the legs passing through the area. For example, there are stricter policies in other areas related to the legs, or the legs are not included in the route plans of OD pairs. In this case, the sulfur emissions remain the same. (ii) The policy obeyed by legs passing through the area is subject to change, such as when the policies in other areas related to that legs are looser, or when the legs are included in one and only one area and is used in the route plans of OD pairs. The sulfur emission will increase under this case. We assume that there exists an OD pair p has only one route plan y and contains only one leg g, which is included in only the area a. For the area a, there are two emission policies (sulfur caps) d_1 and d_2 $(d_1 > d_2)$. And the volume via land and water transportation for the OD pair p under the emission policy d_1 are defined as $\eta_p^L(d_1)$ and $\eta_p^W(d_1)$. The sulfur emission under d_1 is $E_{d_1} = \dot{e}_p^L \cdot \eta_p^L(d_1) + \dot{e}_{gd_1}^W \cdot \eta_p^W(d_1)$, and the sulfur emission under d_2 is $E_{d_2} = \dot{e}_p^L \cdot \eta_p^L(d_2) + \dot{e}_{gd_2}^W \cdot \eta_p^W(d_2)$. Since $\overline{c}_{d_1}^W < \overline{c}_{d_2}^W$, we have $v_{gd_1}^W > v_{gd_2}^W$. Thereby, we get $\eta_p^W(d_1) > \eta_p^W(d_2)$ and $\eta_p^L(d_1) < \eta_p^L(d_2)$. We can derive that $E_{d_1} < E_{d_2}$ since $\dot{e}_{gd_1}^W < \dot{e}_{gd_2}^W$.

In summary, for the area with the least number of leg passes, a stricter emission policy (a smaller sulfur cap) leads to a higher or unchanged total sulfur emission. ■

Appendix B: Proof of Proposition 2

Proposition 2: Given the values of the variables θ_{gd}, if $\max\limits_{y \in Y_p}\left\{\sum_{g \in G_y}\sum_{d \in D} \dot{e}_{gd}^W \theta_{gd}\right\} < \dot{e}_p^L$, M1's objective value is: $\bar{n}_p \dot{e}_p^L - \frac{\bar{n}_p \max\limits_{y \in Y_p}\left\{\sum_{g \in G_y}\sum_{d \in D} v_{gd}^W \theta_{gd} - v_y^{-T}\right\}}{\max\limits_{y \in Y_p}\left\{\sum_{g \in G_y}\sum_{d \in D} v_{gd}^W \theta_{gd} - v_y^{-T}\right\} + v_p^L}\left(\dot{e}_p^L - \sum_{g \in G_y : y = \operatorname{argmax}\limits_{y \in Y_p} v_y^W} \sum_{d \in D} \dot{e}_{gd}^W \theta_{gd}\right)$. The values of decision variable are: $\pi_y = \eta_p^W$ for $y = \operatorname{argmax}\limits_{y \in Y_p}\left\{\sum_{g \in G_y}\sum_{d \in D} v_{gd}^W \theta_{gd} - v_y^{-T}\right\}$ and $\pi_y = 0$ for $y \in Y_p \setminus \left\{\operatorname{argmax}\limits_{y \in Y_p}\left\{\sum_{g \in G_y}\sum_{d \in D} v_{gd}^W \theta_{gd} - v_y^{-T}\right\}\right\}$.

Proof: Because the binary variables θ_{gd} annd β_{ad} are determined, the constraints related to these two variables are omitted. The remainder of the model M1 could be divided into $|P|$ independent sub-problems, each of which is related to an OD pair $p \in P$. In addition, as the value of θ_{gd} is known, we define a parameter $v_y^W = \sum_{g\in G_y}\sum_{d\in D} v_{gd}^W\theta_{gd} - v_y^{-T},\ \forall y \in Y_p$. Then, the sub-problem $\mathrm{M1}_p$ for the OD pair p is shown as follow.

$[\mathbf{M1}_{\boldsymbol{p}}]$ *Minimize* $\dot{e}_p^L\eta_p^L + \sum_{y\in Y_p}\pi_y\left(\sum_{g\in G_y}\sum_{d\in D}\dot{e}_{gd}^W\theta_{gd}\right)$ (B-1)

s.t. $\eta_p^W + \eta_p^L = \bar{n}_p$ (B-2)

$\sum_{y\in Y_p}\pi_y = \eta_p^W$ (B-3)

$\frac{\eta_p^W}{\eta_p^L} = \frac{\gamma_p^W}{v_p^L}$ (B-4)

$\gamma_p^W = \frac{\sum_{y\in Y_p}\pi_y v_y^W}{\sum_{y\in Y_p}\pi_y}$ (B-5)

$\eta_p^W, \eta_p^L, \gamma_p^W \geq 0$ (B-6)

$\pi_y \geq 0 \qquad \forall y \in Y_p$ (B-7)

If $\max_{y\in Y_p}\left\{\sum_{g\in G_y}\sum_{d\in D}\dot{e}_{gd}^W\theta_{gd}\right\} < \dot{e}_p^L$, which means the largest emission of a route plan among all the route plans for the OD pair p is less than the emission of the land transportation for the OD pair, Objective (B-1) is equivalent to minimizing "$\dot{e}_p^L\eta_p^L + \max_{y\in Y_p}\left\{\sum_{g\in G_y}\sum_{d\in D}\dot{e}_{gd}^W\theta_{gd}\right\}\sum_{y\in Y_p}\pi_y$", which is further equivalent to maximizing $\sum_{y\in Y_p}\pi_y$, i.e., η_p^W.

According to (B-4) and v_p^L is a parameter, the variable γ_p^W should be as large as possible. Because $\gamma_p^W = \frac{\sum_{y\in Y_p}\pi_y v_y^W}{\sum_{y\in Y_p}\pi_y} \leq \max_{y\in Y_p} v_y^W$ and $\sum_{y\in Y_p}\pi_y = \eta_p^W$, the value of variable γ_p^W could reach its maximum value, i.e., $\max_{y\in Y_p} v_y^W$, when $\pi_y = \eta_p^W$ for $y = \operatorname{argmax}_{y\in Y_p} v_y^W$ and $\pi_y = 0$ for $y \in Y_p \setminus \{\operatorname{argmax}_{y\in Y_p} v_y^W\}$.

Because of (B-2), (B-4) and $\gamma_p^W = \max_{y\in Y_p} v_y^W$ in the optimal solution,

$\eta_p^W = \frac{\bar{n}_p \max_{y\in Y_p} v_y^W}{\max_{y\in Y_p} v_y^W + v_p^L}$ (B-8)

Then the optimal objective value of the above model $\mathrm{M1}_p$ can be formulated as:

$\dot{e}_p^L\eta_p^L + \sum_{y\in Y_p}\pi_y\left(\sum_{g\in G_y}\sum_{d\in D}\dot{e}_{gd}^W\theta_{gd}\right)$

$= \left(\bar{n}_p - \eta_p^W\right)\dot{e}_p^L + \eta_p^W\sum_{g\in G_y: y=\operatorname{argmax}_{y\in Y_p} v_y^W}\sum_{d\in D}\dot{e}_{gd}^W\theta_{gd}$

$$= \bar{n}_p \dot{e}_p^L - \eta_p^W \left(\dot{e}_p^L - \sum_{g \in G_y : y = \underset{y \in Y_p}{\operatorname{argmax}} v_y^W} \sum_{d \in D} \dot{e}_{gd}^W \theta_{gd} \right)$$

$$= \bar{n}_p \dot{e}_p^L - \frac{\bar{n}_p \max\limits_{y \in Y_p} v_y^W}{\max\limits_{y \in Y_p} v_y^W + v_p^L} \left(\dot{e}_p^L - \sum_{g \in G_y : y = \underset{y \in Y_p}{\operatorname{argmax}} v_y^W} \sum_{d \in D} \dot{e}_{gd}^W \theta_{gd} \right)$$

Recall that $v_y^W = \sum_{g \in G_y} \sum_{d \in D} v_{gd}^W \theta_{gd} - v_y^{-T}, \ \forall y \in Y_p$. For all the OD pairs, the objective value of the original model M1 is formulated as follows.

$$\bar{n}_p \dot{e}_p^L - \frac{\bar{n}_p \max\limits_{y \in Y_p} \left\{ \sum_{g \in G_y} \sum_{d \in D} v_{gd}^W \theta_{gd} - v_y^{-T} \right\}}{\max\limits_{y \in Y_p} \left\{ \sum_{g \in G_y} \sum_{d \in D} v_{gd}^W \theta_{gd} - v_y^{-T} \right\} + v_p^L} \left(\dot{e}_p^L - \sum_{g \in G_y : y = \underset{y \in Y_p}{\operatorname{argmax}} v_y^W} \sum_{d \in D} \dot{e}_{gd}^W \theta_{gd} \right) \quad \text{(B-9)}$$

The values of decision variable are $\pi_y = \eta_p^W$ for $y = \underset{y \in Y_p}{\operatorname{argmax}} \left\{ \sum_{g \in G_y} \sum_{d \in D} v_{gd}^W \theta_{gd} - v_y^{-T} \right\}$ and $\pi_y = 0$ for $y \in Y_p \setminus \left\{ \underset{y \in Y_p}{\operatorname{argmax}} \left\{ \sum_{g \in G_y} \sum_{d \in D} v_{gd}^W \theta_{gd} - v_y^{-T} \right\} \right\}$.■

Appendix C: Proof of Proposition 3

Proposition 3: Given the values of the variables θ_{gd}, if $\min\limits_{y \in Y_p} \left\{ \sum_{g \in G_y} \sum_{d \in D} \dot{e}_{gd}^W \theta_{gd} \right\} > \dot{e}_p^L$, M1's objective value is: $\bar{n}_p \dot{e}_p^L - \frac{\bar{n}_p \min\limits_{y \in Y_p} \left\{ \sum_{g \in G_y} \sum_{d \in D} v_{gd}^W \theta_{gd} - v_y^{-T} \right\}}{\min\limits_{y \in Y_p} \left\{ \sum_{g \in G_y} \sum_{d \in D} v_{gd}^W \theta_{gd} - v_y^{-T} \right\} + v_p^L} \left(\dot{e}_p^L - \sum_{g \in G_y : y = \underset{y \in Y_p}{\operatorname{argmin}} v_y^W} \sum_{d \in D} \dot{e}_{gd}^W \theta_{gd} \right)$.

The values of decision variable are: $\pi_y = \eta_p^W$ for $y = \underset{y \in Y_p}{\operatorname{argmin}} \left\{ \sum_{g \in G_y} \sum_{d \in D} v_{gd}^W \theta_{gd} - v_y^{-T} \right\}$ and $\pi_y = 0$ for $y \in Y_p \setminus \left\{ \underset{y \in Y_p}{\operatorname{argmin}} \left\{ \sum_{g \in G_y} \sum_{d \in D} v_{gd}^W \theta_{gd} - v_y^{-T} \right\} \right\}$.

Proof: Similar as the proof of the Proposition 1, the sub-problem is the same as the model $\mathrm{M1}_p$.

If $\min\limits_{y \in Y_p} \left\{ \sum_{g \in G_y} \sum_{d \in D} \dot{e}_{gd}^W \theta_{gd} \right\} > \dot{e}_p^L$, which means the least emission of a route plan among all the route plans for the OD pair p is greater than the emission of the land transportation for the OD pair, Objective (B-1) is equivalent to minimizing "$\dot{e}_p^L \eta_p^L + \min\limits_{y \in Y_p} \left\{ \sum_{g \in G_y} \sum_{d \in D} \dot{e}_{gd}^W \theta_{gd} \right\} \sum_{y \in Y_p} \pi_y$", which is further equivalent to minimizing $\sum_{y \in Y_p} \pi_y$, i.e., η_p^W.

Because $\gamma_p^W = \frac{\sum_{y \in Y_p} \pi_y v_y^W}{\sum_{y \in Y_p} \pi_y} \geq \min\limits_{y \in Y_p} v_y^W$ and $\sum_{y \in Y_p} \pi_y = \eta_p^W$, the value of variable γ_p^W could reach its minimum value, i.e., $\min\limits_{y \in Y_p} v_y^W$, when $\pi_y = \eta_p^W$ for $y = \underset{y \in Y_p}{\operatorname{argmin}} v_y^W$ and $\pi_y = 0$ for $y \in Y_p \setminus \{\underset{y \in Y_p}{\operatorname{argmin}} v_y^W\}$.

Because of (B-2), (B-4) and $\gamma_p^W = \min\limits_{y \in Y_p} v_y^W$ in the optimal solution

$$\eta_p^W = \frac{\bar{n}_p \min\limits_{y\in Y_p} v_y^W}{\min\limits_{y\in Y_p} v_y^W + v_p^L} \quad \text{(C-1)}$$

Then the optimal objective value of the above model $\mathrm{M1}_p$ can be formulated as:

$$\dot{e}_p^L \eta_p^L + \sum_{y\in Y_p} \pi_y \left(\sum_{g\in G_y} \sum_{d\in D} \dot{e}_{gd}^W \theta_{gd} \right)$$

$$= \left(\bar{n}_p - \eta_p^W\right)\dot{e}_p^L + \eta_p^W \sum_{g\in G_y : y = \operatorname{argmin}\limits_{y\in Y_p} v_y^W} \sum_{d\in D} \dot{e}_{gd}^W \theta_{gd}$$

$$= \bar{n}_p \dot{e}_p^L - \eta_p^W \left(\dot{e}_p^L - \sum_{g\in G_y : y = \operatorname{argmin}\limits_{y\in Y_p} v_y^W} \sum_{d\in D} \dot{e}_{gd}^W \theta_{gd} \right)$$

$$= \bar{n}_p \dot{e}_p^L - \frac{\bar{n}_p \min\limits_{y\in Y_p} v_y^W}{\min\limits_{y\in Y_p} v_y^W + v_p^L} \left(\dot{e}_p^L - \sum_{g\in G_y : y = \operatorname{argmin}\limits_{y\in Y_p} v_y^W} \sum_{d\in D} \dot{e}_{gd}^W \theta_{gd} \right)$$

Recall that $v_y^W = \sum_{g\in G_y} \sum_{d\in D} v_{gd}^W \theta_{gd} - v_y^{-T},\ \forall y \in Y_p$. For all the OD pairs, the objective value of the original model $\mathrm{M1}$ is formulated as follows.

$$\bar{n}_p \dot{e}_p^L - \frac{\bar{n}_p \min\limits_{y\in Y_p} \left\{ \sum_{g\in G_y} \sum_{d\in D} v_{gd}^W \theta_{gd} - v_y^{-T} \right\}}{\min\limits_{y\in Y_p} \left\{ \sum_{g\in G_y} \sum_{d\in D} v_{gd}^W \theta_{gd} - v_y^{-T} \right\} + v_p^L} \left(\dot{e}_p^L - \sum_{g\in G_y : y = \operatorname{argmin}\limits_{y\in Y_p} v_y^W} \sum_{d\in D} \dot{e}_{gd}^W \theta_{gd} \right) \quad \text{(C-2)}$$

The values of decision variable are $\pi_y = \eta_p^W$ for $y = \operatorname{argmin}\limits_{y\in Y_p} \left\{ \sum_{g\in G_y} \sum_{d\in D} v_{gd}^W \theta_{gd} - v_y^{-T} \right\}$ and $\pi_y = 0$ for $y \in Y_p \setminus \left\{ \operatorname{argmin}\limits_{y\in Y_p} \left\{ \sum_{g\in G_y} \sum_{d\in D} v_{gd}^W \theta_{gd} - v_y^{-T} \right\} \right\}$.■

Appendix D: Proof of Proposition 4

Proposition 4: Given the values of the variables θ_{gd}, for each OD pair p, the maximum and minimum emission of a route plan is calculated as follows:

$\min\limits_{y\in Y_p} \left\{ \sum_{g\in G_y} \sum_{d\in D} \dot{e}_{gd}^W \theta_{gd} \right\} = \dot{e}_{gd}^W$, g is the longest leg for the OD pair p, d is the highest degree among all the emission control degrees of areas that this leg covers.

$\max\limits_{y\in Y_p} \left\{ \sum_{g\in G_y} \sum_{d\in D} \dot{e}_{gd}^W \theta_{gd} \right\} = \sum_{g\in \bar{G}_p} \sum_{d\in D} \dot{e}_{gd}^W \theta_{gd}$, $\bar{G}_p$ is the set of legs that constitute the OD pair p, and each leg is included in one and only one area.

Proof: For an OD pair, the minimum emission of the water transportation is in the case that the whole process is under as high degree (strict) of emission control policy as possible. The above case exists in a route plan which contains just one leg from the origin to the destination without any transshipment. Then the whole process is under the highest degree among all the emission control degrees that are related to the areas the OD pair (i.e., the leg) covers. For the example in Figure 2, the route plan 1 contains just one leg; and the whole process is under the highest emission control degree, i.e., sulfur cap 0.1%. Then the emission of this route plan is the lowest among all the route plans for the OD pair.

Therefore, $\min_{y \in Y_p} \left\{ \sum_{g \in G_y} \sum_{d \in D} \dot{e}_{gd}^{W} \theta_{gd} \right\} = \dot{e}_{gd}^{W}$. Here leg g in "$\dot{e}_{gd}^{W}$" is the longest leg for the OD pair p; degree d in "$\dot{e}_{gd}^{W}$" is the highest degree among all the emission control degrees of areas that this leg covers.

For an OD pair, the maximum emission of the water transportation is in the case that the whole process is under as low degree of emission control policy as possible. It implies there is none part of a leg that would be under a low emission control degree but is under a high emission control degree. If a leg covers two or more areas with different emission control degrees, the leg must be executed according to the highest degree among these different emission control degrees. When above mentioned case is avoided, the emission of a route plan for the OD pair could reach its maximum value. For the example in Figure 2, the route plan 4 contains four legs, which exactly fit the four areas with four different emission control degrees. In other words, each one of the four legs is included in exactly one area. Then the emission of this route plan is the highest among all the route plans for the OD pair. Therefore, $\max_{y \in Y_p} \left\{ \sum_{g \in G_y} \sum_{d \in D} \dot{e}_{gd}^{W} \theta_{gd} \right\} = \sum_{g \in \bar{G}_p} \sum_{d \in D} \dot{e}_{gd}^{W} \theta_{gd}$. Here $\bar{G}_p$ is the set of legs that constitute the OD pair p, and each leg is included in one and only one area. ■

References

Buchem, M., Golak, J. A. P., & Grigoriev, A. (2022) Vessel velocity decisions in inland waterway transportation under uncertainty. *European Journal of Operational Research* 296(2): 669–678.

Chang, Y. T., Roh, Y., & Park, H. (2014) Assessing noxious gases of vessel operations in a potential Emission Control Area. *Transportation Research Part D: Transport and Environment 28*: 91–97.

Chua, Y. J., Soudagar, I., Ng, S. H., & Meng, Q. (2023) Impact analysis of environmental policies on shipping fleet planning under demand uncertainty. *Transportation Research Part D: Transport and Environment* 120: 103744.

Duan, L., Tavasszy, L. A., & Rezaei, J. (2019) Freight service network design with heterogeneous preferences for transport time and reliability. *Transportation Research Part E: Logistics and Transportation Review* 124: 1–12.

Fan, Y., Behdani, B., Bloemhof-Ruwaard, J. & Zuidwijk, R. (2019) Flow consolidation in hinterland container transport: An analysis for perishable and dry cargo. *Transportation Research Part E: Logistics and Transportation Review* 130: 128–160.

Gao, Z., Huang, H., Guo, J., Yang, L., & Wu, J. (2023) Future urban transport management. *Frontiers of Engineering Management*, in press.

Gang, D. & Lee, P. T. W. (2020) Environmental effects of emission control areas and reduced speed zones on container ship operation. *Journal of Cleaner Production* 274: 122582.

Gong, X., & Li, Z.-C. (2022) Determination of subsidy and emission control coverage under competition and cooperation of China-Europe Railway Express and liner shipping. *Transport Policy* 125: 323–335.

Hoen, K. M. R., Tan, T., Fransoo, J. C. & Houtum, G. J. (2014) Effect of carbon emission regulations on transport mode selection under stochastic demand. *Flexible Services and Manufacturing Journal* 26(1-2): 170–195.

Hu, Q., Gu, W., & Wang, S. A. (2022). Optimal subsidy scheme design for promoting intermodal freight transport. *Transportation Research Part E: Logistics and Transportation Review* 157: 102561.

Joseph, L., Giles, T., Nishatabbas, R., & Tristan, S. (2021) A techno-economic environmental cost model for Arctic shipping. *Transportation Research Part A: Policy and Practice* 151: 28–51.

Khakdaman M., Rezaei J., & Tavasszy L. A. (2020) Shippers' willingness to delegate modal control in freight transportation. *Transportation Research Part E: Logistics and Transportation Review* 141: 102027.

Kong, Q., Jiang, C., & Ng, A. K. Y. (2021) The economic impacts of restricting black carbon emissions on cargo shipping in the Polar Code Area. *Transportation Research Part A: Policy and Practice* 147: 159–176.

Li, Z. C., & Sheng, D. (2016) Forecasting passenger travel demand for air and high-speed rail integration service: A case study of Beijing-Guangzhou corridor, China. *Transportation Research Part A: Policy and Practice* 94: 397-410.

Ling, S., Ma, S., & Jia, N. (2022) Sustainable urban transportation development in China: A behavioral perspective. *Frontiers of Engineering Management* 9: 16-30.

Liu, B., Wang, Y., Li, Z.-C., & Zheng, J. (2023) An exact method for vessel emission monitoring with a ship-deployed heterogeneous fleet of drones. *Transportation Research Part C: Emerging Technologies* 153: 104198.

Meng, L., Liu, K., He, J., Han, C., & Liu, P. (2022) Carbon emission reduction behavior strategies in the shipping industry under government regulation: A tripartite evolutionary game analysis. *Journal of Cleaner Production* 378: 134556.

Palak, G., Ekşioğlu, S. D. & Geunes, J. (2014) Analyzing the impacts of carbon regulatory mechanisms on supplier and mode selection decisions: An application to a biofuel supply chain. *International Journal of Production Economics* 154: 198–216.

Ship and Bunker (2023) World bunker prices. https://shipandbunker.com/prices. Accessed in June 2023.

Sun, Y., Yang, L., & Zheng, J. (2020) Emission control areas: More or fewer? *Transportation Research Part D: Transport and Environment* 84: 102349.

Svindland, M. (2018) The environmental effects of Emission Control Area regulations on short sea shipping in Northern Europe: The case of container feeder vessels. *Transportation Research Part D: Transport and Environment* 61: 423-430.

Tan, Z., Zeng, X., Shao, S., Chen, J., & Wang, H. (2022a) Scrubber installation and green fuel for inland river ships with non-identical streamflow. *Transportation Research Part E: Logistics and Transportation Review* 161: 102677.

Tan, Z., Zhang, M., Shao, S., Liang, J., & Sheng, D. (2022b) Evasion strategy for a coastal cargo ship with unpunctual arrival penalty under sulfur emission regulation. *Transportation Research Part E: Logistics and Transportation Review* 164: 102818.

Wang, K., Yin, M., & Ayisi, A. D. (2023) Effects of reduced speed on the benefits and pollution of Yangtze River ships. *Transportation Research Record* 2677(6): 783–796.

Wang, S., Zhen, L., & Psaraftis, H. N. (2021) Three potential benefits of the EU and IMO's landmark efforts to monitor carbon dioxide emissions from shipping. *Frontiers of Engineering Management* 8(2): 310–311.

Yan, X., Wang, K., Yuan, Y., Jiang, X., & Negenborn, R. R. (2018) Energy-efficient shipping: An application of big data analysis for optimizing engine speed of inland ships considering multiple environmental factors. *Ocean Engineering* 169: 457–468.

Yuan, Y. L., Yang, M., Feng, T., Rasouli, S., Ruan, X. P., Wang, X. Y., & Li, Y. (2022) Analyzing heterogeneity in passenger satisfaction, loyalty, and complaints with air-rail integrated services. *Transportation Research Part E: Logistics and Transportation Review* 164: 102827.

Zhang, Q., Zheng, Z., Wan, Z., & Zheng, S. (2020) Does emission control area policy reduce sulfur dioxides concentration in Shanghai? *Transportation Research Part D: Transport and Environment* 81: 102289.

Zhang, Y., Sun, L., Fan, T., Ma, F., & Xiong, Y. (2023) Speed and energy optimization method for the inland all-electric ships in battery-swapping mode. *Ocean Engineering* 284: 115234.

Zhen, L., Hu, Z., Yan, R., Zhuge, D., & Wang, S. (2020) Route and speed optimization for liner ships under emission control policies. *Transportation Research Part C: Emerging Technologies* 110: 330-345.

Zhen, L., Wang, W., & Lin, S. (2022) Analytical comparison on two incentive policies for shore power equipped ships in berthing activities. *Transportation Research Part E: Logistics and Transportation Review* 161: 102686.

Zhuge, D., Wang, S., Zhen, L., & Laporte, G. (2021) Subsidy design in a vessel speed reduction incentive program under government policies. *Naval Research Logistics* 68(3): 344–358.

1 Zis, T. P. V. (2019) Prospects of cold ironing as an emissions reduction option. *Transportation Research*
2 *Part A: Policy and Practice* 119: 82–95.
3 Zis, T. P. V., Psaraftis, H. N., Panagakos, G., & Kronbak, J. (2019) Policy measures to avert possible
4 modal shifts caused by sulphur regulation in the European Ro-Ro sector. *Transportation Research*
5 *Part D: Transport and Environment* 70: 1–17.